Probing the Nature of Neutrinos: the Search for Neutrinoless Double-β Decay

Junting Huang

Shanghai Jiao Tong University

July 21, 2023

Vietnam School on Neutrinos

ICISE center, Quy Nhon, VN

Table of Contents

Neutrinos in the Standard Model

- proposed in 1930, Pauli
- discovered in 1956, reactor $\overline{\nu}_e$, Cowan and Reines
- Lee, Yang, Wu in 1956–1957: parity violation
- Goldhaber in 1957: neutrinos are left-handed
- three light active neutrinos ν_e, ν_μ, and ν_τ
- $N = 2.9840 \pm 0.0082$ from Z boson decay
- neutrinos were considered massless in Standard Model

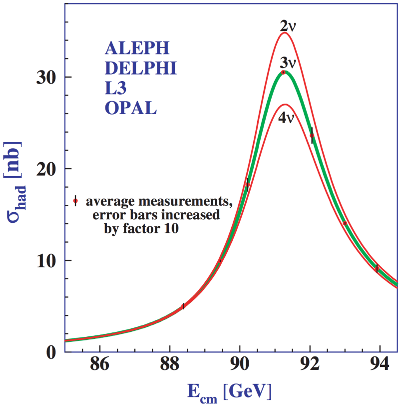

Number of active neutrino flavors from Z decay in LEP experiments.

Discovery of Neutrino Oscillations

- Super-Kamiokande: atmospheric ν_μ disappearance
- SNO: ν_e flux and total neutrino $\nu_{e,\mu,\tau}$ flux from the Sun
- neutrinos have non-zero mass, 2015 Nobel Prize

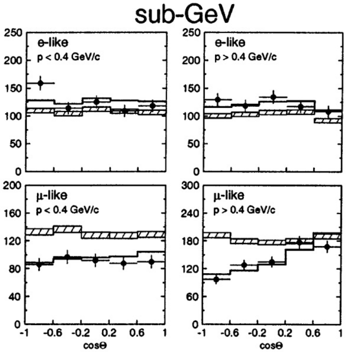

(a) Super-Kamiokande, 1998 [1]

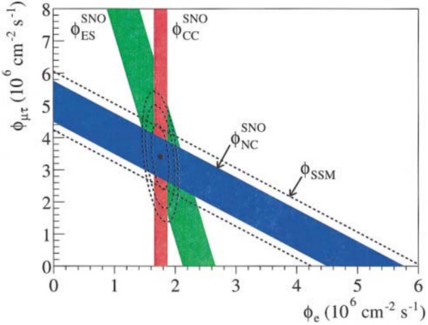

(b) SNO, 2002 [2]

Neutrino Oscillation Measurements

- ν_α: state with specific flavor (ν_e, ν_μ, ν_τ)
- ν_i: state with specific mass (m_1, m_2, m_3)
- $|\nu_\alpha\rangle = \sum_i U^*_{\alpha i}|\nu_i\rangle$, matrix U is unitary, called PMNS matrix

$$U = \begin{pmatrix} 1 & & \\ & c_{23} & s_{23} \\ & -s_{23} & c_{23} \end{pmatrix} \begin{pmatrix} c_{13} & & -s_{13}e^{i\delta_{CP}} \\ & 1 & \\ -s_{13}e^{i\delta_{CP}} & & c_{13} \end{pmatrix} \begin{pmatrix} c_{12} & s_{12} & \\ -s_{12} & c_{12} & \\ & & 1 \end{pmatrix}$$

- θ_{ij}, δ_{CP}, $\Delta m^2_{ij} = m_i^2 - m_j^2$
- θ_{12}, Δm^2_{21} (solar, reactor)
- θ_{23}, $\left|\Delta m^2_{32}\right|$ (atmo., beam)
- θ_{13} (reactor)
- $\left|\Delta m^2_{32}\right| = 2.5 \times 10^{-3}\,\mathrm{eV}^2$
  $\Delta m^2_{21} = 7.5 \times 10^{-5}\,\mathrm{eV}^2$
- mass ordering and absolute masses remain unknown

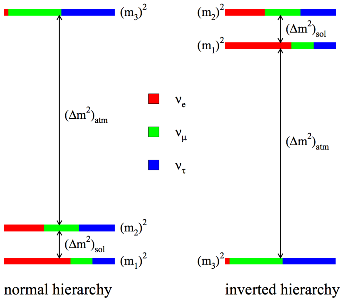

Absolute Neutrino Masses

- KATRIN experiment [3]
  - end point of tritium β decay at 18.57 keV
  - $m_\beta^2 = \sum |U_{ei}|^2 m_i^2$
  - $m_\beta < 1.1\,\text{eV}$, 2019 [3]
  - $m_\beta < 0.8\,\text{eV}$, 2021 [4]
- cosmology, Planck data
  - e.g. $\sum m_i < 0.28\,\text{eV}$ [5]
  - cosmological model dependent

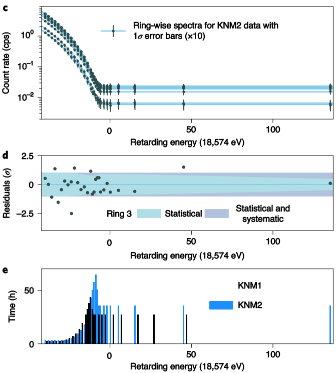

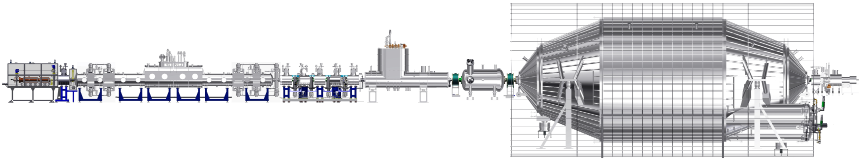

Where Do Neutrino Masses Come from? [11]

- neutrinos can be Dirac particles: $m\overline{\psi}_R\psi_L$, need ψ_R

- why are neutrino masses so small?

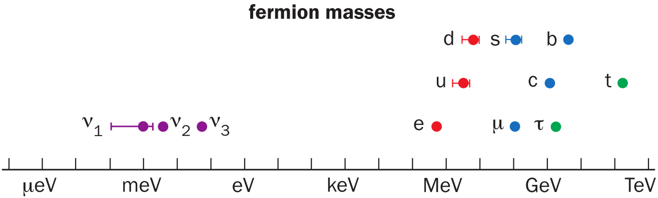

- a different possible source: seesaw mechanism [6–10]

- seesaw requires that neutrinos are Majorana particles

Majorana Neutrinos

- Majorana in 1937: $\nu = \overline{\nu}$ [12]

$$(i\widetilde{\gamma}^{\mu}\partial_{\mu} - m)\widetilde{\psi} = 0,$$

where $\widetilde{\gamma}^{\mu}$ are purely imaginary satisfying Clifford Algebra, $i\widetilde{\gamma}^{\mu}$ is real, $\widetilde{\psi}$ is a real field [13]

"The theory, however, can be obviously modified so that the β-emission, both positive and negative, is always accompanied by the emission of a neutrino."
— E. Majorana [12]

- besides neutrino mass, may also help explain baryon asymmetry: leptogenesis [14], L violation induces B violation
- most promising probe: neutrinoless double-β decay

Neutrinoless Double-β Decay

- double-β ($2\nu\beta\beta$) decay
  - first calculated by Goeppert-Mayer in 1935
  - first direct observation: $^{82}\mathrm{Se} \to {}^{82}\mathrm{Kr} + 2e^- + 2\overline{\nu}$ in a time projection chamber (TPC), Elliott, Hahn, and Moe, 1987
- neutrinoless double-β ($0\nu\beta\beta$) decay, Furry, 1939, lepton number violation process, Majorana $\leftrightarrow$ $0\nu\beta\beta$ decay [15]

$$^{A}_{Z}\mathrm{X} \to {}^{\;\;A}_{Z+2}\mathrm{X} + 2e^-$$

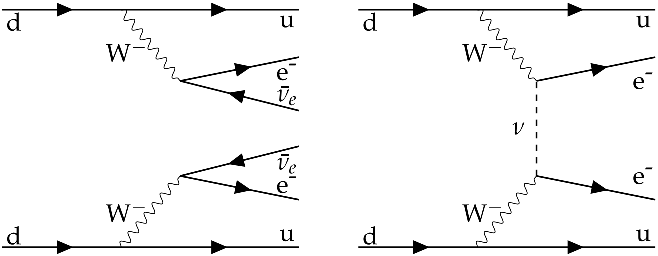

Feynman diagrams of $2\nu\beta\beta$ and $0\nu\beta\beta$ decays.

Decay Half-Life

- decay half-life

$$\frac{1}{T_{1/2}} = G^{0\nu}\left|M^{0\nu}\right|^2 \frac{m_{\beta\beta}^2}{m_e^2}.$$

  - phase factor $G^{0\nu}$, nuclear matrix element $M^{0\nu}$
  - effective Majorana mass $m_{\beta\beta} = \left|\sum_k U_{ek}^2 m_k\right|$
- $m_{\beta\beta}$ vs. mass ordering and absolute neutrino mass

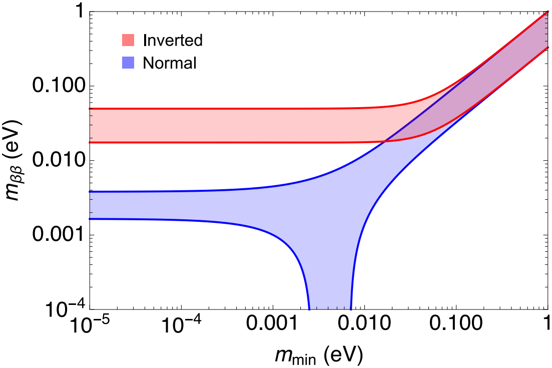

Experimental Design

Signal Signature

- mono-energetic peak at $Q_{\beta\beta}$
- background free

$$T_{1/2} \propto \epsilon M t$$

where M is mass, t is running time, ϵ is efficiency

- with background

$$T_{1/2} \propto \epsilon \sqrt{\frac{Mt}{B \Delta E}}$$

  - B: background index, in $\text{keV}^{-1}\,\text{kg}^{-1}\,\text{yr}^{-1}$
  - ΔE: energy resolution

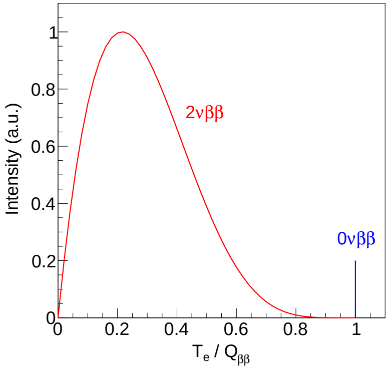

The two-electron energy spectrum for the $2\nu\beta\beta$ and $0\nu\beta\beta$ decays. For example, $Q_{\beta\beta} = 2039.06$ keV for ^{76}Ge.

Intrinsic $2\nu\beta\beta$ Background

- $T^{2\nu}_{1/2} \ll T^{0\nu}_{1/2}$, $2\nu\beta\beta$ decay is a potential ultimate background
- the fraction of the $2\nu\beta\beta$ counts in the peak region [16]

$$F \propto (\Delta E/Q_{\beta\beta})^6$$

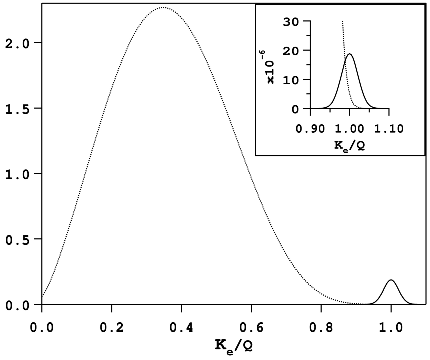

Signature of $0\nu\beta\beta$ decay in the observed spectrum of electron energy normalized by the Q value ($Q_{\beta\beta}$) [16].

Choice of Isotopes

- high abundance: lower cost in enrichment, or without enrichment, e.g. ^{130}Te
- high $Q_{\beta\beta}$: low intrinsic $2\nu\beta\beta$ background, low background of radioactivity

isotope	natural abundance (%)	$Q_{\beta\beta}$(MeV)
^{48}Ca	0.187	4.263
^{76}Ge	7.8	2.039
^{82}Se	8.7	2.998
^{96}Zr	2.8	3.348
^{100}Mo	9.8	3.035
^{116}Cd	7.5	2.813
^{130}Te	34.08	2.527
^{136}Xe	8.9	2.459
^{150}Nd	5.6	3.371

Nuclear Matrix Element and Phase Space Factor

- larger $\left|M^{0\nu}\right|^2$ and $G^{0\nu}$, easier for $0\nu\beta\beta$ decay to happen

$$1/T_{1/2} = G^{0\nu}\left|M^{0\nu}\right|^2 m_{\beta\beta}^2/m_e^2$$

- uncertainty in $\left|M^{0\nu}\right|^2$ due to nuclear models

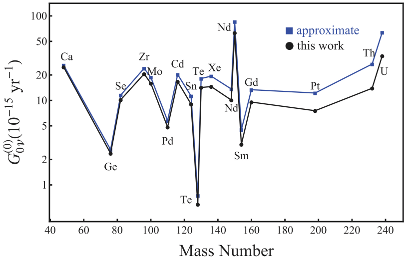

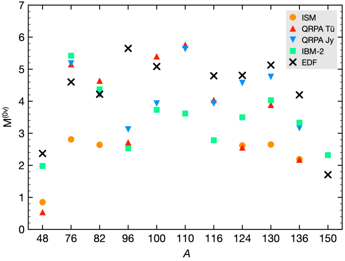

Phase factors [17] and nuclear matrix elements [18].

Background Challenges

- cosmic rays and cosmogenic activation, e.g. ^{77}Ge, ^{137}Xe
- radioactivity of detector materials, e.g. ^{238}U, ^{232}Th, ^{60}Co
- anthropogenic, e.g. ^{137}Cs, ^{110m}Ag
- neutrinos: $\nu + e^- \rightarrow \nu + e^-$

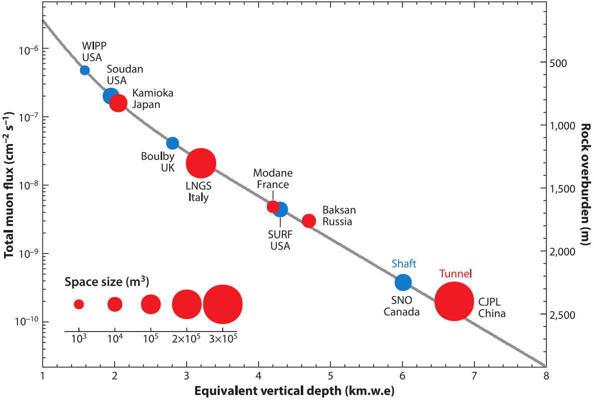

World underground laboratories [19].

Experimental Programs

Main Approaches

- source $\neq$ detector
  - source on a foil
  - event energy and topology
  - low resolution and efficiency
- source = calorimeter
  - measure double-β energy
  - high resolution and efficiency
  - no event topology
- source = calorimeter = tracker
  - high pressure gas TPC
  - high efficiency and resolution, event topology
  - large volume, weak self-shielding

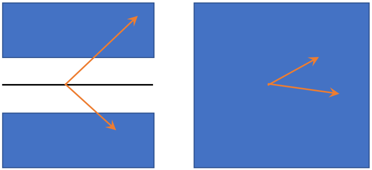

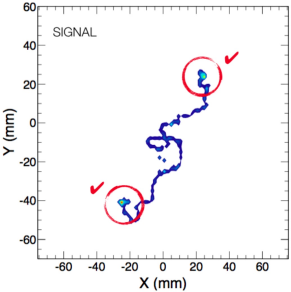

Bottom figure taken from [20] based on simulation.

Detector Signals

- signals come in form of heat (bolometer), light (scintillator), and charge (semiconductor, etc.)
- non-exhaustive list, selectively introduce them clockwise

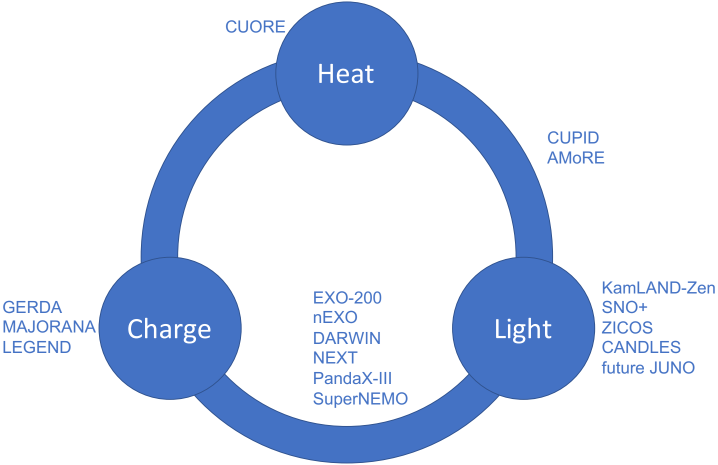

CUORE Experiment

- Cryogenic Underground Observatory for Rare Events, at LNGS
- bolometers, ultra-cold $^{130}TeO_2$
- 988 TeO_2 crystals, 206 kg of ^{130}Te, 11.8 mK
- 7 keV FWHM at $Q_{\beta\beta}$

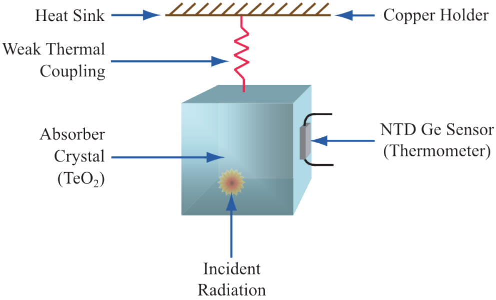

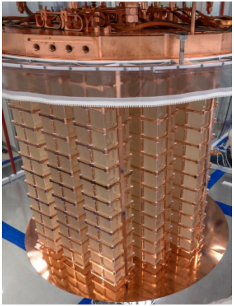

CUORE 2022 Results

- Nature 2022: $T_{1/2} > 2.2 \times 10^{25}$ yr [21]
- 1 t yr exposure, background 1.49×10^{-2} keV^{-1} kg^{-1} yr^{-1}
- 90% background near $Q_{\beta\beta}$ from α, ^{60}Co peak at 2505.7 keV

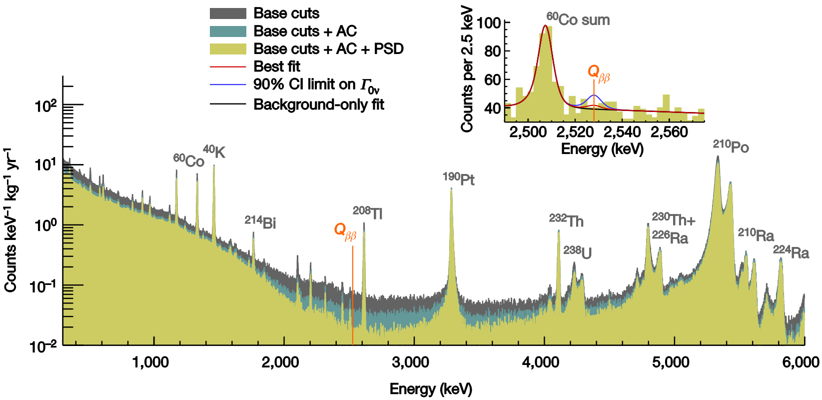

CUPID Experiment

- CUPID: CUORE Upgrade with Particle Identification
- separate α from β/γ with the same energy
- CUPID-0: scintillating bolometers $Zn^{82}Se$ crystals
- CUPID-Mo: $Li_2{}^{100}MoO_4$, chosen for CUPID ton-scale
- PRL 126, 181802 (2021), 1.17 kg yr, 7.6 keV FWHM

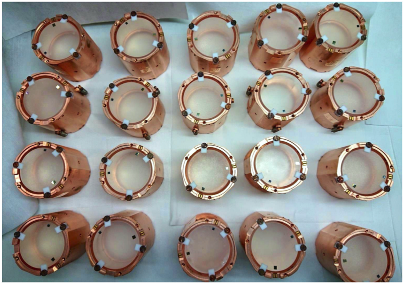

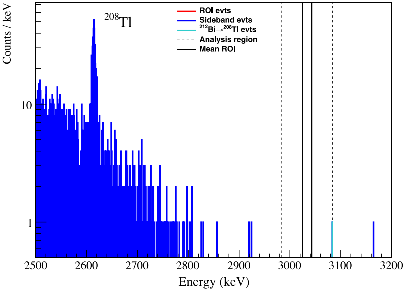

KamLAND-Zen

- multi-ton scale experiment, light from liquid scintillator
- liquid scintillator loaded with 3.1% Xe, 745 kg, 91% enriched
- ^{110m}Ag from Fukushima (2011)
- 270 keV FWHM

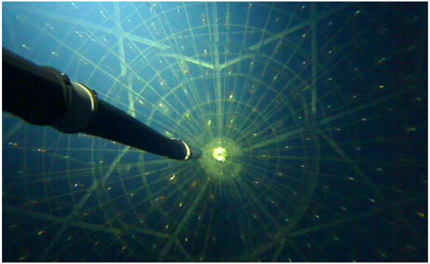

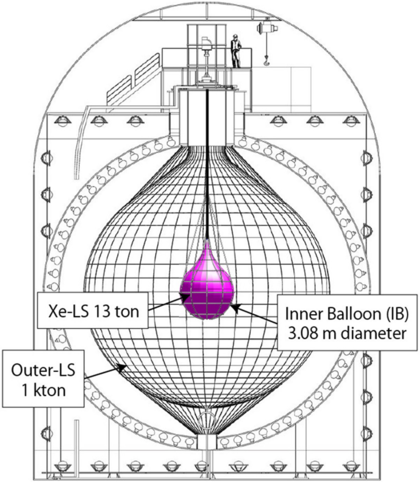

1879 17-inch and 20-inch PMTs

Kamland-Zen in 2022 Results

- $T_{1/2} > 2.3 \times 10^{26}$ yr at 90% C.L., world leading [22]
- entering inverted mass ordering region!

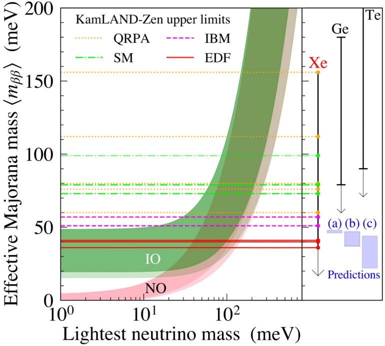

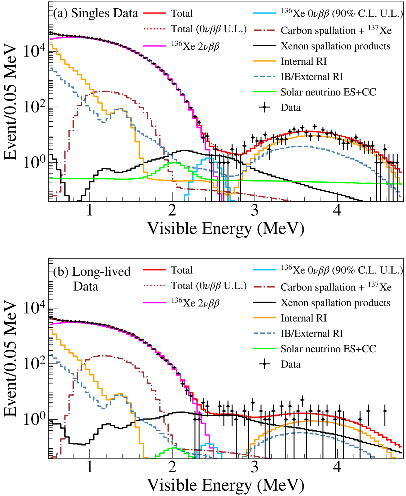

SNO+

- SNOLAB, 5890 mwe
- 780 tons liquid scintillator loaded with 0.5% natural Te, about 1300 kg ^{130}Te
- 7000 tons water for shielding, $\sim$ 9300 PMTs

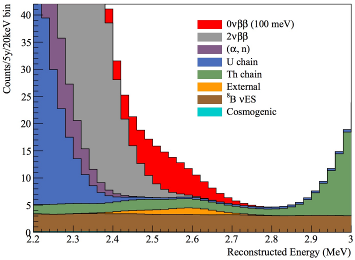

Expected spectrum [23].

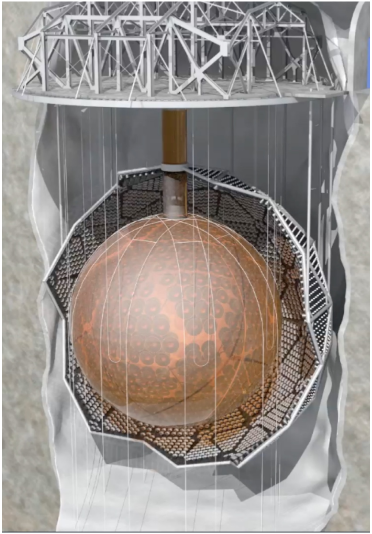

EXO-200, nEXO, DARWIN, PandaX-30T

- liquid Xe TPC
- EXO-200 (Enriched Xenon Observatory)
  - 110 kg of Xe, enriched to 80.6% in ^{136}Xe
  - finished, PRL 123, 161802 (2019), 67 keV FWHM
- nEXO (next EXO), plann to use 5 ton of Xe, barium tagging
- DARWIN: 50t Xe for dark matter searches, 3.6t of ^{136}Xe [24]
- PandaX-30T, expect similar sensitivity

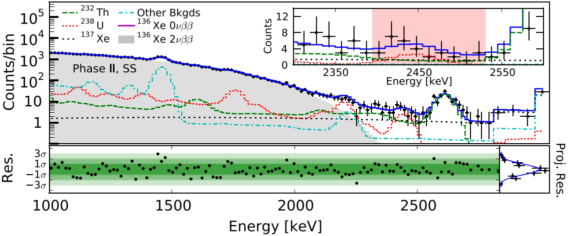

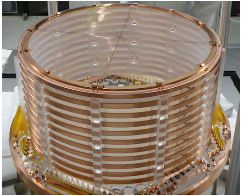

NEXT and PandaX-III

- high pressure gas Xe TPC: high resolution ($< 25\,\text{keV}$ FWHM), topology to reject α, β and γ
- NEXT: electroluminescent amplification + PMTs
  - NEXT-White: 5 kg Xe at 15 bar
  - NEXT-100: 100 kg, under construction
- PandaX-III: fine-pitch Micromegas, running a 20 kg prototype at 5 bar, aim for 200 kg modules

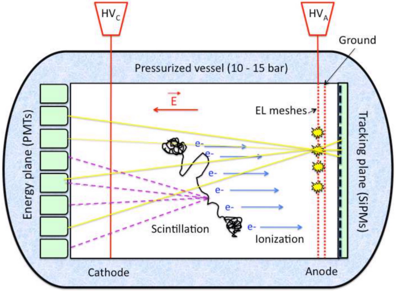

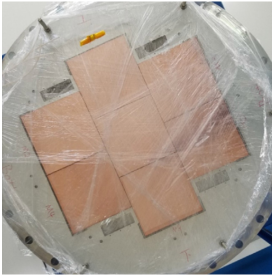

SuperNEMO

- built upon the success of NEMO-3
- thin foil enriched in double-β isotope, flexibility in isotope type
- wire-chamber tracker: measure particles' trajectories, background rejection
- segmented calorimeter: energy and timing

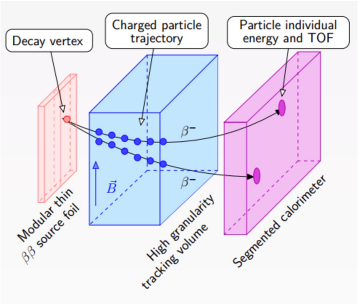

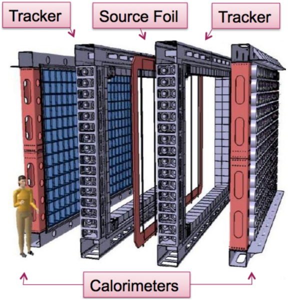

GERDA, MAJORANA, and LEGEND

- $^{76}\mathrm{Ge} \rightarrow {}^{76}\mathrm{Se} + 2e^{-}$
- source is also detector, high efficiency
- best energy resolution and lowest background index in all $0\nu\beta\beta$ decay experiments
- commercial technology, modest cryogenic requirements

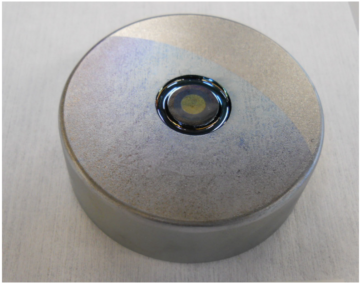

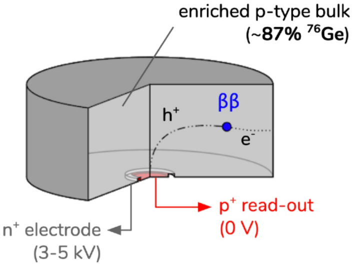

GERDA Experiment

- LNGS, Italy, 3500 wme, 10^6 reduction of cosmic rays
- water tank: 10 m diameter, muon veto, shielding
- LAr veto: 0.5 m diameter, 2 m high, veto, shielding, cooling
- about 40 detectors, enriched to about 87%, 35.6 kg

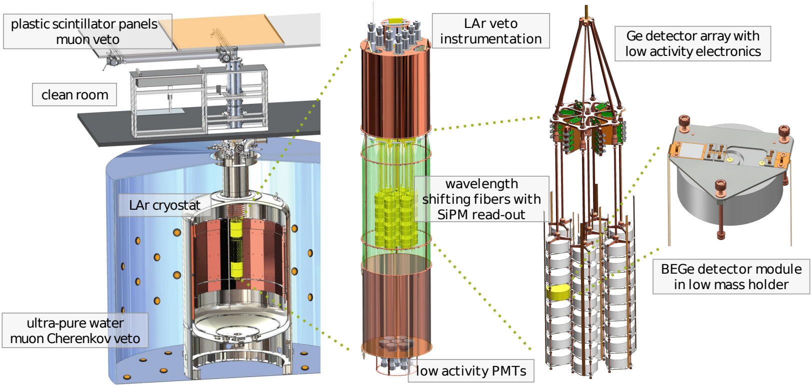

Detector Array and Liquid Argon Veto Instrumentation

- detectors mounted on 6 strings, nylon cylinder
- liquid argon veto: TPB reflector, PMTs, wavelength shifting fibers + SiPMs

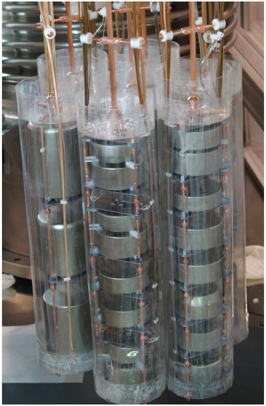
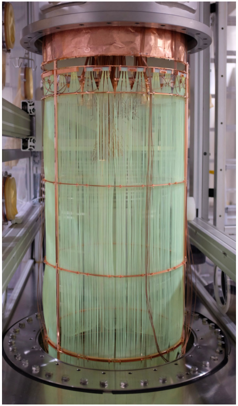
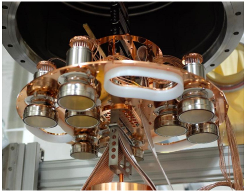
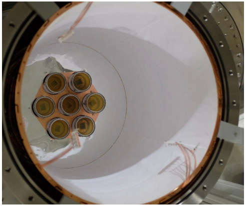

Energy Calibration

- ^{228}Th, weekly calibration
- between calibrations: test pulses injected every 20 s, stable operating conditions for physics analysis is about 80%

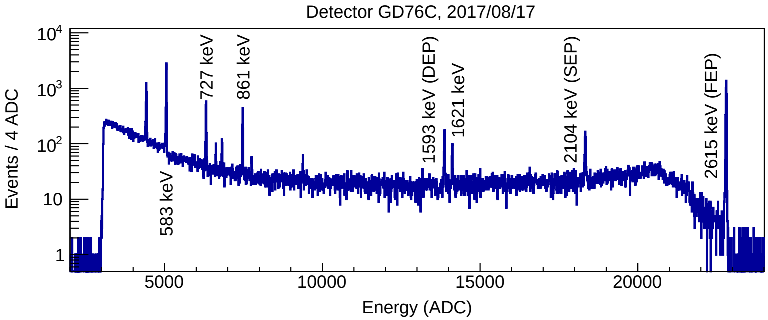

An example of the GERDA Phase II calibration data.

Calibration Curve

- after each calibration, find the position of the gamma lines
- fit a linear function as the calibration curve (ADC to keV)
- energy resolution determined from width of Gaussian

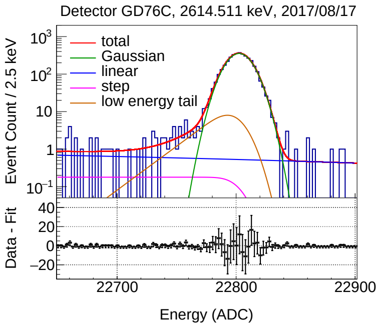

(a) fit to full energy peak

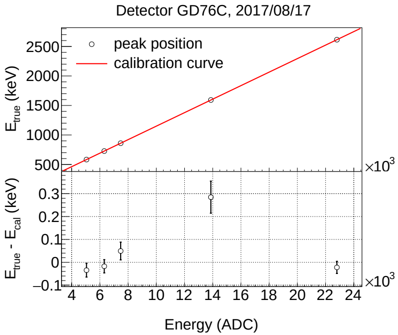

(b) calibration curve

Energy Resolutions

- resolution changes over time due to hardware changes
- partition the dataset based on stability, one resolution for each of the partition

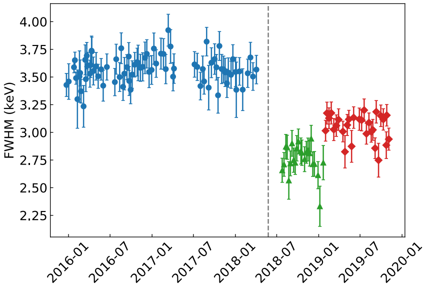

(a) resolution jumps

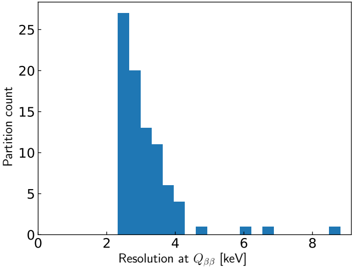

(b) resolution distribution

Background Reduction

- liquid argon veto + pulse shape discrimination + cosmic veto
- first in the field to operate in background-free regime
- signal efficiency: 46% for coaxial, 61% for BEGe, 66% for IC

$\beta\beta$ decay signal: single-site event energy deposition in a 1 mm^3 volume

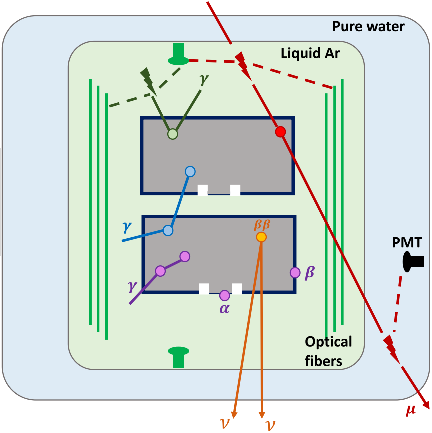

Pulse shape discrimination (PSD) for multi-site and surface α, β events

Ge detector anti-coincidence

LAr veto based on Ar scintillation light read by fibers and PMT

Muon veto based on Cherenkov light and plastic scintillator

Pulse Shape Discrimination

- A is the maximum current amplitude, E is the energy
- too small A/E: multi-site and n^+ electrode
- too large A/E: p^+ electrode

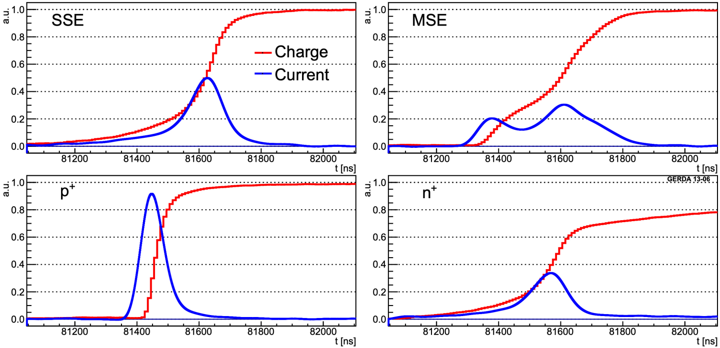

Candidate pulse traces taken from data for a single-site event (SSE), multi-site event (MSE), p^+ electrode event and n^+ surface event [25].

Energy Spectrum

- analysis cut: liquid argon veto, pulse shape discrimination
- at low energy, dominated by $2\nu\beta\beta$ decay of ^{76}Ge
- $Q_{\beta\beta} \pm 25\,\text{keV}$ for blind analysis

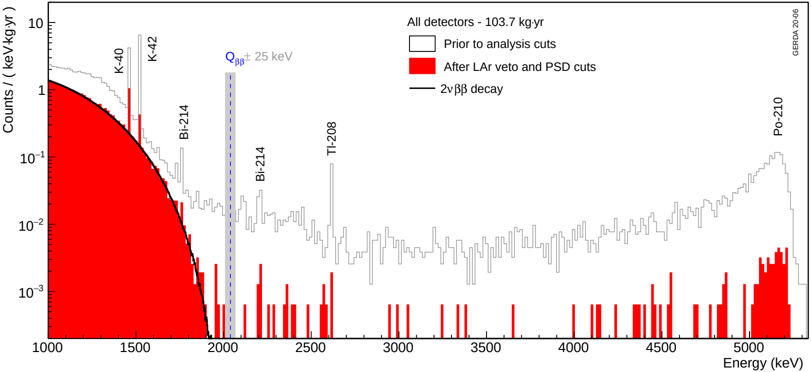

Calibrated energy spectrum after all event selections.

Final GERDA Results: PRL 125 (2020), 252502

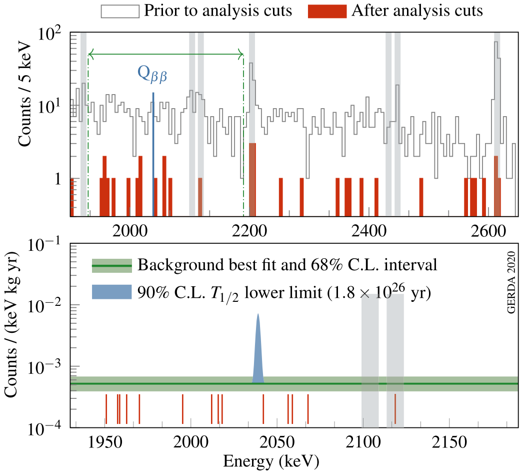

- half-life limit: $T_{1/2} > 1.8 \times 10^{26}$ yr at 90% C.L.
- world's lowest background: $B = 5.2 \times 10^{-4}$ cts/(keV kg yr)

Comparison: Background vs. Exposure

- keys to $0\nu\beta\beta$ experiments: background and exposure
- extreme background requirements for LEGEND, nEXO, etc.

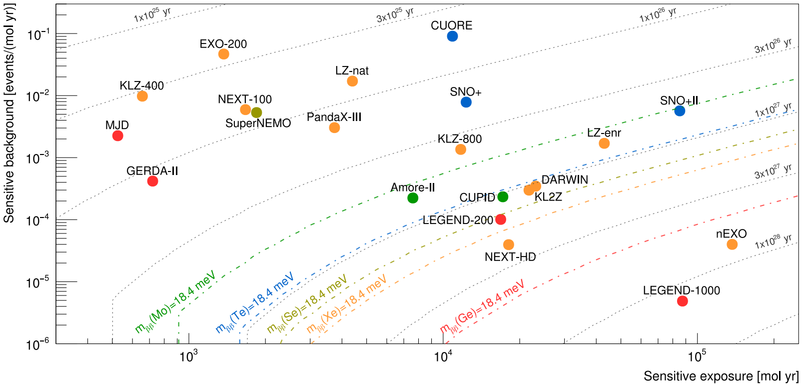

A summary of background and exposure for various experiments [26].

Current Status

- leading constraints on $m_{\beta\beta}$ comes from ^{76}Ge, ^{130}Te, and ^{136}Xe
- region above the inverted mass ordering is mostly excluded

isotope	experiment	year	half-life limit (yr)	$m_{\beta\beta}$ (meV)	reference
^{75}Ge	GERDA	2020	1.8×10^{26}	79-180	[27]
^{136}Xe	KamLAND-Zen	2022	2.3×10^{26}	36-156	[22]
^{136}Xe	EXO	2019	3.5×10^{25}	93-286	[28]
^{130}Te	CUORE	2022	2.2×10^{25}	90-305	[21]

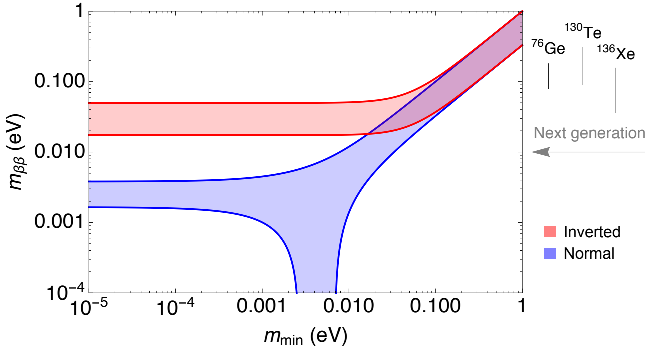

Future Prospect

- cover inverted ordering region: $m_{\beta\beta} \sim 10\,\text{meV}$, use larger mass, further reduce background
- CUPID, nEXO, KamLAND2-Zen, NEXT, etc.
- LEGEND: 1 ton of ^{76}Ge, run for 10 yr, 10^{28} yr, first phase LEGEND-200 with 200 kg ^{76}Ge is ongoing at LNGS

LEGEND-1000
1000 kg, $T_{1/2} > 10^{28}$

LEGEND-200
200 kg, $T_{1/2} > 10^{27}$

GERDA/MAJORANA
30 kg, $T_{1/2} > 10^{26}$

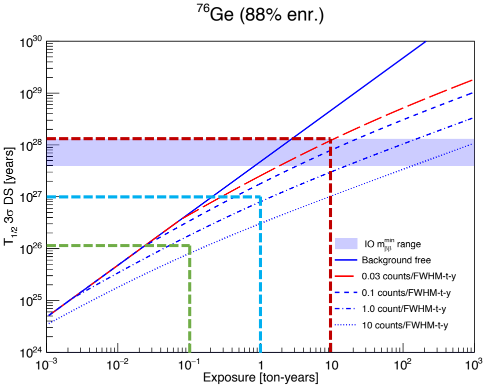

Future Projects in China

- PandaX-III, PandaX-30T (SJTU): xenon TPC [29, 30]
- JUNO (IHEP): load ^{136}Xe or ^{130}Te in liquid scintillator [31]
- CUPID-China (Fudan) [32], CDEX (Tsinghua) [33], and NvDEx (IMP) [34]

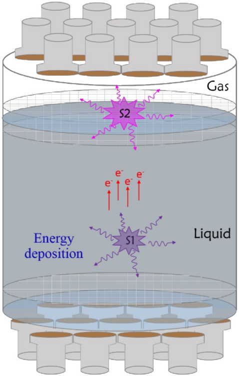

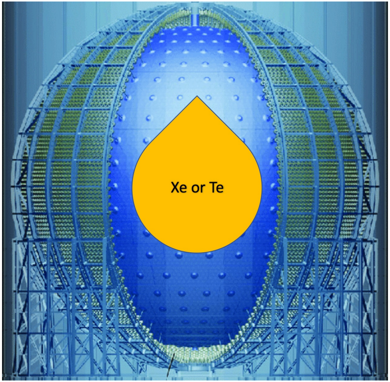

Relation with Other Neutrino Experiments

- mass ordering measurement
  - NOvA + T2K: no preference with 2020 results [35]
  - JUNO: data taking starts in 2023, 6 years, 3-4σ
  - DUNE: $> 5\sigma$, 1.2 MW beam in 2026 with 20 kt mass (1/2)
- precision measurement of mixing parameters [36]
- absolute mass from beta decay, sum of neutrino masses

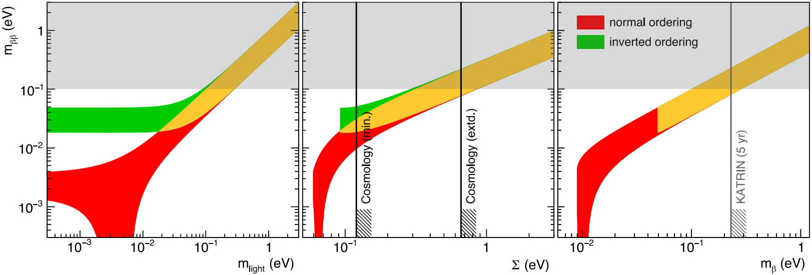

Figure adapted from [37].

Summary and Outlook

- Majorana neutrinos may solve several fundamental issues in particle physics and cosmology
  - origin of neutrino mass, why it is small
  - why the universe is dominated by matter
- neutrinoless double-β decay is the most promising probe
  - keys: exposure, energy resolution, and background
  - technologies: bolometers, scintillators, TPCs, semiconductors
- most of the parameter space above the inverted mass ordering region are excluded, results led by ^{76}Ge, ^{130}Te, and ^{136}Xe
- the goal of next generation experiment is to reach below the inverted mass ordering region, ton-scale, lower background

References I

[1] Y. Fukuda et al., "Evidence for oscillation of atmospheric neutrinos", Phys.Rev.Lett. **81**, 1562–1567 (1998).

[2] Q. Ahmad et al., "Direct evidence for neutrino flavor transformation from neutral current interactions in the Sudbury Neutrino Observatory", Phys.Rev.Lett. **89**, 011301 (2002).

[3] M. Aker et al., "Improved Upper Limit on the Neutrino Mass from a Direct Kinematic Method by KATRIN", Phys. Rev. Lett. **123**, 221802 (2019).

[4] M. Aker et al., "Direct neutrino-mass measurement with sub-electronvolt sensitivity", Nature Phys. **18**, 160–166 (2022).

[5] S. Roy Choudhury and S. Choubey, "Updated Bounds on Sum of Neutrino Masses in Various Cosmological Scenarios", JCAP **09**, 017 (2018).

References II

[6] P. Minkowski, "$\mu \to e\gamma$ at a Rate of One Out of 10^9 Muon Decays?", Phys. Lett. B **67**, 421–428 (1977).

[7] T. Yanagida, "Proc. workshop on unified theory and the baryon number in the universe", KEK Report No. 79-18 **95** (1979).

[8] M. Gell-Mann, P. Ramond, and R. Slansky, "Complex Spinors and Unified Theories", Conf. Proc. C **790927**, 315–321 (1979).

[9] S. L. Glashow, "The Future of Elementary Particle Physics", NATO Sci. Ser. B **61**, 687 (1980).

[10] R. N. Mohapatra and G. Senjanovic, "Neutrino Mass and Spontaneous Parity Nonconservation", Phys. Rev. Lett. **44**, 912 (1980).

[11] H. Murayama, "The origin of neutrino mass", Phys. World **15**, 35–39 (2002).

References III

[12] E. Majorana, "Teoria simmetrica dell'elettrone e del positrone", Nuovo Cim. **14**, 171–184 (1937).

[13] F. Wilczek, "Majorana returns", Nature Physics **5**, 614–618 (2009).

[14] M. Fukugita and T. Yanagida, "Baryogenesis Without Grand Unification", Phys. Lett. B **174**, 45–47 (1986).

[15] S. Bilenky and C. Giunti, "Neutrinoless Double-Beta Decay: a Probe of Physics Beyond the Standard Model", Int. J. Mod. Phys. A **30**, 1530001 (2015).

[16] S. R. Elliott and P. Vogel, "Double beta decay", Ann. Rev. Nucl. Part. Sci. **52**, 115–151 (2002).

[17] J. Kotila and F. Iachello, "Phase space factors for double-β decay", Phys. Rev. C **85**, 034316 (2012).

References IV

[18] J. Gómez-Cadenas and J. Martín-Albo, "Phenomenology of neutrinoless double beta decay", PoS **GSSI14**, 004 (2015).

[19] J.-P. Cheng et al., "The China Jinping Underground Laboratory and its Early Science", Ann. Rev. Nucl. Part. Sci. **67**, 231–251 (2017).

[20] P. Ferrario et al., "Demonstration of the event identification capabilities of the NEXT-White detector", JHEP **10**, 052 (2019).

[21] D. Q. Adams et al., "Search for Majorana neutrinos exploiting millikelvin cryogenics with CUORE", Nature **604**, 53–58 (2022).

[22] S. Abe et al., "First Search for the Majorana Nature of Neutrinos in the Inverted Mass Ordering Region with KamLAND-Zen", (2022).

[23] *Sno+ homepage*, `https://falcon.phy.queensu.ca/SNO+/index.html`.

References V

[24] F. Agostini et al., "Sensitivity of the DARWIN observatory to the neutrinoless double beta decay of ^{136}Xe", Eur. Phys. J. C **80**, 808 (2020).

[25] M. Agostini et al., "Pulse shape discrimination for GERDA Phase I data", Eur. Phys. J. C **73**, 2583 (2013).

[26] M. Agostini, G. Benato, J. A. Detwiler, J. Menéndez, and F. Vissani, "Toward the discovery of matter creation with neutrinoless double-beta decay", (2022).

[27] M. Agostini et al., "Final Results of GERDA on the Search for Neutrinoless Double-β Decay", Phys. Rev. Lett. **125**, 252502 (2020).

[28] G. Anton et al., "Search for Neutrinoless Double-β Decay with the Complete EXO-200 Dataset", Phys. Rev. Lett. **123**, 161802 (2019).

References VI

[29] X. Chen et al., "PandaX-III: Searching for neutrinoless double beta decay with high pressure ^{136}Xe gas time projection chambers", Sci. China Phys. Mech. Astron. **60**, 061011 (2017).

[30] K. Ni et al., "Searching for neutrino-less double beta decay of ^{136}Xe with PandaX-II liquid xenon detector", Chin. Phys. C **43**, 113001 (2019).

[31] J. Zhao, L.-J. Wen, Y.-F. Wang, and J. Cao, "Physics potential of searching for $0\nu\beta\beta$ decays in JUNO", Chin. Phys. C **41**, 053001 (2017).

[32] A. Giuliani, J. J. Gomez Cadenas, S. Pascoli, E. Previtali, R. Saakyan, K. Schäffner, and S. Schönert, "Double Beta Decay APPEC Committee Report", (2019).

[33] W. H. Dai et al., "Search for Neutrinoless Double-Beta Decay of ^{76}Ge with a Natural Broad Energy Germanium Detector", (2022).

References VII

[34] Y. Mei, X. Sun, and N. Xu, "Topmetal CMOS direct charge sensing plane for neutrinoless double-beta decay search in high-pressure gaseous TPC", (2020).

[35] K. J. Kelly, P. A. N. Machado, S. J. Parke, Y. F. Perez-Gonzalez, and R. Z. Funchal, "Neutrino mass ordering in light of recent data", Phys. Rev. D **103**, 013004 (2021).

[36] S.-F. Ge and W. Rodejohann, "JUNO and Neutrinoless Double Beta Decay", Phys. Rev. D **92**, 093006 (2015).

[37] M. Agostini et al., "Probing Majorana neutrinos with double-β decay", Science **365**, 1445 (2019).